ICARUS 34, 486–495 (1978)

Exploratory Experiments of Impact Craters Formed in Viscous-Liquid Targets: Analogs for Martian Rampart Craters?

DONALD E. GAULT

Murphys Center of Planetology, Murphys, California 95247

AND

RONALD GREELEY

Department of Geology and Center for Meteorite Studies, Arizona State University, Tempe, Arizona 85281

Received September 2, 1977; revised November 29, 1977

Exploratory experimental impact studies have been performed using "soupy" mud as a target material. Although differing in details, the results appear to support the hypothesis that ejecta deposits around a class of Martian craters recently revealed in high-resolution Viking Orbiter images were emplaced as a flow of fluidized materials.

INTRODUCTION

One of the most striking results of the Viking Orbiter images is the discovery of craters for which ejecta deposits appear to have been emplaced at least partly by flow of fluidized materials (Carr *et al.*, 1976, 1977). The ejecta for this class of crater has pronounced scarps and/or ridges on its outer boundaries, and the large craters are characterized by multiple-tiered continuous ejecta deposits extending as far as two crater diameters from the crater rim (Fig. 1). Craters of this type were first recognized in the Mariner 9 images and termed rampart craters (McCauley, 1973), their peculiar morphology being attributed to modulation of the ejecta deposits by eolian processes (McCauley, 1973; Arvidson *et al.*, 1976). Although it is clear in many cases that eolian erosion has been effective, the improved resolution of the Viking Orbiter images has provided convincing photogeological evidence that in many instances ejecta materials were emplaced as a ground-hugging flow which was probably first transported ballistically from the crater and then subsequently slid along the ground surface before coming to a final resting position. Because craters with this unique ejecta morphology are not observed on the Moon or Mercury, we believe (as suggested by Carr *et al.*, 1976, 1977; and Head and Roth, 1976), that either subsurface water and/or ice, or the Martian atmosphere are accountable for the unusual ejecta deposits. At the time of impact, the ejecta was transformed into a fluidized sheet, either as a result of entrained water, melted and vaporized ice, or entrapped atmospheric gas.

Experimental studies of impact cratering in rocks and particulates have proven invaluable in the past for the understanding and interpretation of the "dry" lunar (and

0019-1035/78/0343-0486$02.00/0

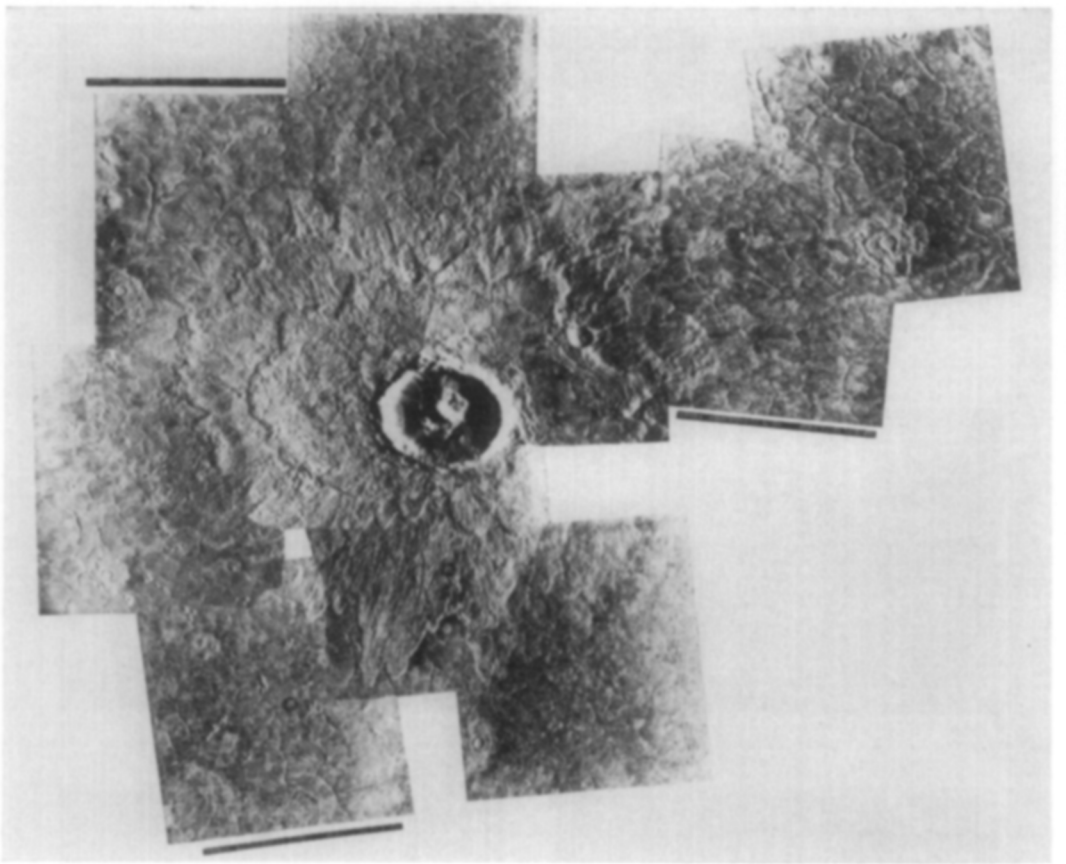

FIG. 1. Mosaic of the Martian crater Arandes (28 km diameter; 43°, 14°). Two distinct ejecta deposits surround the crater, one extending as much as two crater diameters from the rim, and a second overlying unit extending out more than a crater diameter. Both units exhibit well-developed scarps along their outer margins; surface morphologies are suggestive of ejecta flow across the surrounding fractured plains.

Mercurian) surface (e.g., Gault *et al.*, 1966, 1972, 1974; Quaide and Oberbeck, 1968; Oberbeck *et al.*, 1974; Stöffler *et al.*, 1975). There are, however, no comparable studies of cratering in liquid media that are applicable to the inferred Martian conditions, and for this reason, very limited and cursory impact studies were undertaken using "soupy" mud targets. The intent of these tests was to explore qualitatively the experimental feasibility and suitable target media prior to initiating a more quantitative and comprehensive study. Because these exploratory experiments provide some interesting substance for the hypothesis of a fluidized ejecta deposition process, this short note has been prepared to present the "first look" results.

EXPERIMENTAL PROCEDURES

The experiments were performed using the facilities of the NASA–Ames Research Center's Vertical Gun Ballistic Range (Gault *et al.*, 1968). Pyrex glass spheres (3.175- and 6.35-mm diameter) were launched with a nominal velocity of 1.8 km/sec at normal incidence into mud targets which were contained in buckets 60 cm in diameter and 20.5 cm deep. The use of Pyrex was predicated on attaining

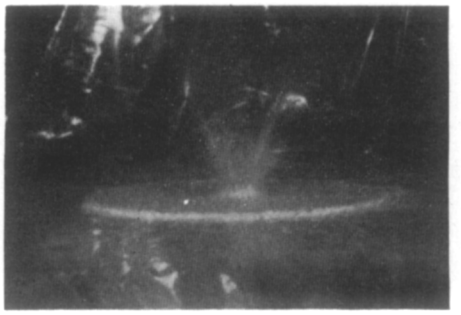

t = 0

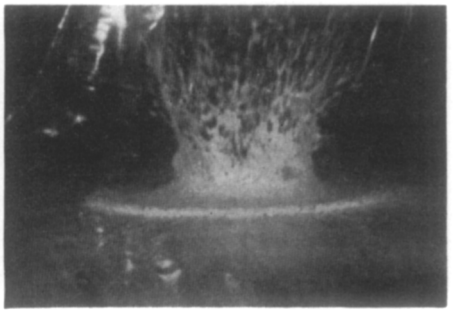

t = 22.5

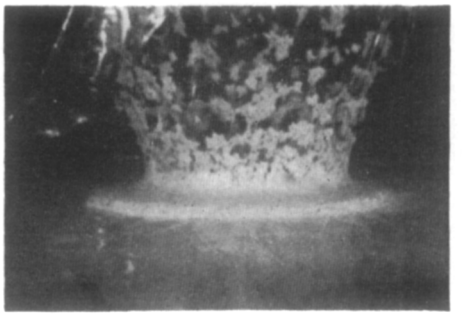

t = 77.5

t = 400

t = 402.5

t = 410

t = 425

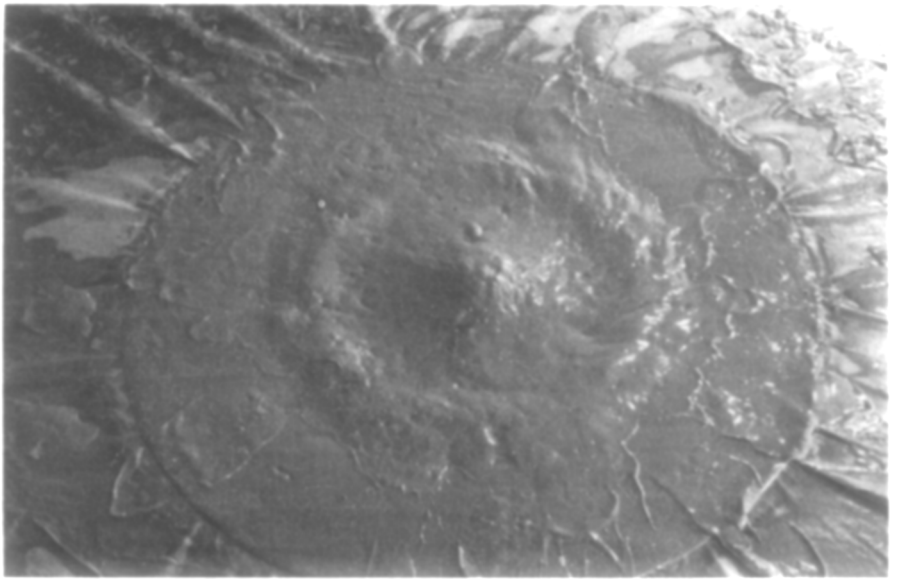

FIG. 3. Crater produced by the impact of a 3.175-mm diameter Pyrex sphere at normal incidence with a velocity of 1.6 km/sec in mud with consistency of honey (Round VGP 1601). Note flow in continuous deposits surrounding crater. The residual central peak was formed as the result of collapse of the original crater of excavation, which was larger and deeper than the final form shown shown here. The prominent ridges radial to crater in upper left and lower right of picture are wrinkles in polyethylene sheet used to cover and protect the reference surface around the target bucket.

complete crushing and disruption of the projectile for the low impact velocities involved in the experiments and, thus, simulated projectile destruction and phenomena of high speed impacts more typical of planetary events. The mud target materials were homogeneous mixtures of potter's clay and water. No quantitative measurements of target viscosities or other physical properties were obtained for these initial exploratory tests, but qualitatively the consistency of the target materials varied from that similar to a thick, wet concrete to a much more fluid substance typified by honey or syrup. Impacts were also performed into water targets as the limiting condition for minimum target viscosity. For these experiments, 1.59-mm-diameter Pyrex spheres were launched with a velocity of 2.5 km/sec into 50-mm-deep water contained in a cubical-shaped tank measuring 1 m on a side. Air pressure in the impact chamber was maintained at 50 mm Hg (approx). Sixteen-millimeter movie records of the impacts were obtained using Millikan cameras operating at a rate of 400 frames/sec.

RESULTS

Selected frames from a 16-mm movie record of one of the impacts into mud are

Fig. 2. Selected frames from a 16-mm movie record of a 6.35-mm-diameter Pyrex sphere impacting a mud target at normal incidence with a velocity of 1.90 km/sec (Round VGP 1599). Note the development and breakup of the conical ejecta plume into small fragments as the crater grows in size, and the mode of secondary cratering by the large fragment shown in the lower right of the last three frames in the sequence. Target mud had consistency of honey. Time t shown in milliseconds after impact.

presented in Fig. 2 to illustrate the general characteristics and essential features of the cratering sequence and ejecta deposition. Upon contact and penetration of the projectile into the target, a thin, conical (almost cylindrical) plume of mud was sprayed up from the walls of the incipient crater. The plume was initially relatively intact with few holes or tears, but as the diameter of the developing cavity increased the ejecta plume broke up into thin, irregular sheets of mud. These sheets represent pieces produced as the result of random tearing and breakup of the plume as it expanded radially outward from the point of impact. Sizes of the individual pieces varied inversely with their ejection velocity. The smallest pieces were ejected first with the highest velocities, and as the incipient crater frew in size, the fragment dimensions increased and ejection velocities decreased. The terminal stage of ejection, when the rim and continuous deposits were formed, was accomplished with an essentially intact sheet of ejecta, but which exhibited radial and subradial tears and cracks.

Although the general details of the ejection processes were independent of target properties, the final crater, the breakup and mode of emplacement of fragments, and the final morphology of the secondary deposits depended on the viscosity of the target medium. Initial results using the largest spheres (6.35 mm) impacting into the wet, concrete-like mud produced well-defined craters with rim diameters of 36 to 38 cm, and there was little or no evidence of flow in either the continuous deposits or the individual ejecta fragments (within approximately one meter of the crater as limited by the wall of the impact chamber). However, changing to a target material of lower viscosity with the consistency of honey or syrups totally changed the character of the ejecta deposits and, at the same time, necessitated reducing the projectile size in order to contain the crater within the bucket. With reduced viscosity of target medium, the resistance against deformation during growth of the crater and deposition of the ejecta was also reduced. As a result, less kinetic energy was required to form the crater (i.e., smaller projectile) and, for a given ejection velocity (i.e., secondary cratering kinetic energy) greater deformation of the ejecta during secondary impact occurred.

With the smaller (3.175 mm) spheres impacting into the honey-like mud, crater diameters were approximately 30 cm. The conical plume remained intact for a longer period of time, broke into smaller sizes, and there was clear evidence of radial flow both in the continuous deposits and the individual secondary fragments (Fig. 3). The mode of emplacing the ejecta fragments is of particular interest and is illustrated schematically in Fig. 4. In part (a) the developing cavity is shown in cross section with the breakup of the ejecta plume shown and the trajectory of a single fragment depicted. Material in the upper part of the fragment (with the greater velocity) is ejected prior to the material in the lower portion (with the lowest velocity); the upper tip of the fragment has a ballistic range R_1 which is greater than that for the lower tip, R_2. Figure 4b illustrates a typical shape for the sheets torn out of the conical ejecta plume, although many highly irregular and contorted shapes also occurred. The remarkable characteristics of the ballistic transport of most of the fragments is shown in Fig. 4c, that is, the fragments experienced little, if any, rotational disturbances caused by tearing and breaking of the ejecta plume and typically impacted the surface (secondary cratering) steeply inclined to the surface as illustrated by Fig. 4d with the same orientation as initially ejected. As a consequence of their orientation, the lower portion of the fragments returned to the surface first and some material "squirted" or flowed along the surface ahead of the remaining portion

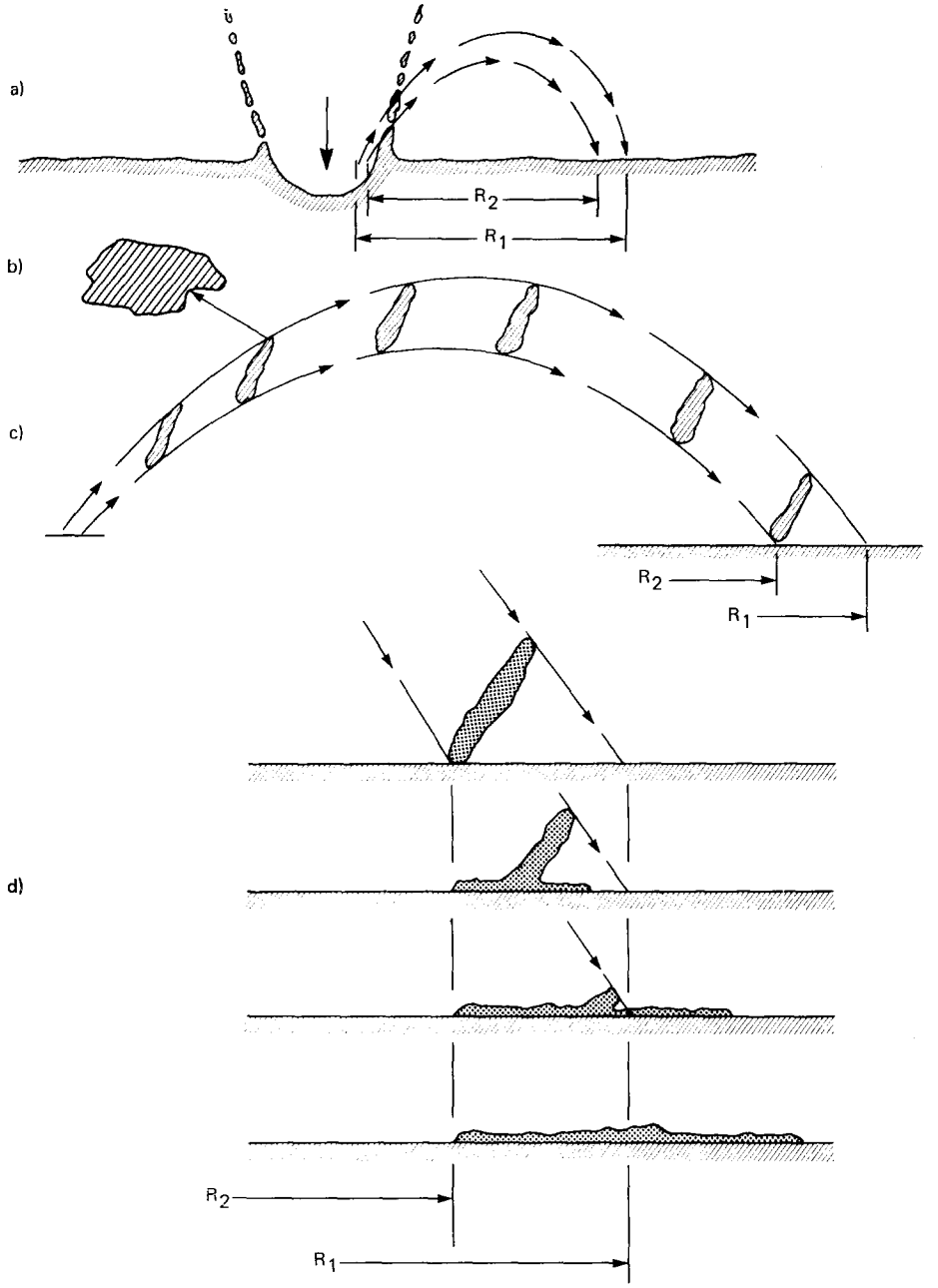

FIG. 4. Schematic representation of the ejection, ballistic transport, and mode of secondary "cratering" by fragments from craters formed in mud.

of the fragment that was still in ballistic transport. The final deposit of the secondary fragment displays two flow fronts, one associated with the initial flow that was triggered by material first deposited at R_2 and a second front associated with the higher velocity fraction of the ejecta deposited closer to R_1. Morphologically the

FIG. 5. Ejecta fragment with apparent episodic flow units formed as result of impact shown in Fig. 2. The three prominent ridges are wrinkles in the protective polyethylene sheet overlying the reference surface.

secondary deposits appear to be the result of two (or more) separate and distinct flow events, the first and largest episode of flow (associated with deposition at R_2) lying stratigraphically below a smaller and "younger" flow episode (associated with deposition near, but downrange from R_1). Figure 5 is an example of one of these "episodic" flows.

Further reduction of target viscosity to the minimum value of water required further reduction in projectile size to 1.59-mm diameter in order to contain the crater within the target water tank. Although it is difficult to define a crater diameter in water, the transient cavities were about 40 cm (Fig. 6); thus, with an expenditure of projectile kinetic energy smaller by a factor of 30 the reduced viscosity of the water resulted in craters of approximately the same size as those produced in the more viscous thick, wet, concrete-like mud. Most significantly the conical ejecta plume remained intact within the geometric limits of the 1-m tank with only one or two (sometimes none) tears or holes appearing in the plume. The "continuous" ejecta deposits for the transient craters, therefore, extended at least to the limits of the walls of the water tank approximately 30 cm beyond the "rims" of the transient craters.

DISCUSSION

These exploratory experiments of impact cratering in viscous materials are believed to support the hypothesis of ejecta fluidization and, although differing in details, the characteristics of the new class of craters revealed by the Viking Orbiter images. A major uncertainty in the application of the observations to Martian conditions is, of course, the validity of extrapolating the results of small-scale experiments to structures with dimensions of tens of kilometers. In this respect the soupy muds are not (nor were they intended to be) a suitable medium for modeling the undisturbed and prefluidized physical properties of the Martian target material(s). Their use precludes, for example, formation and preservation of interior terraces and steep slopes

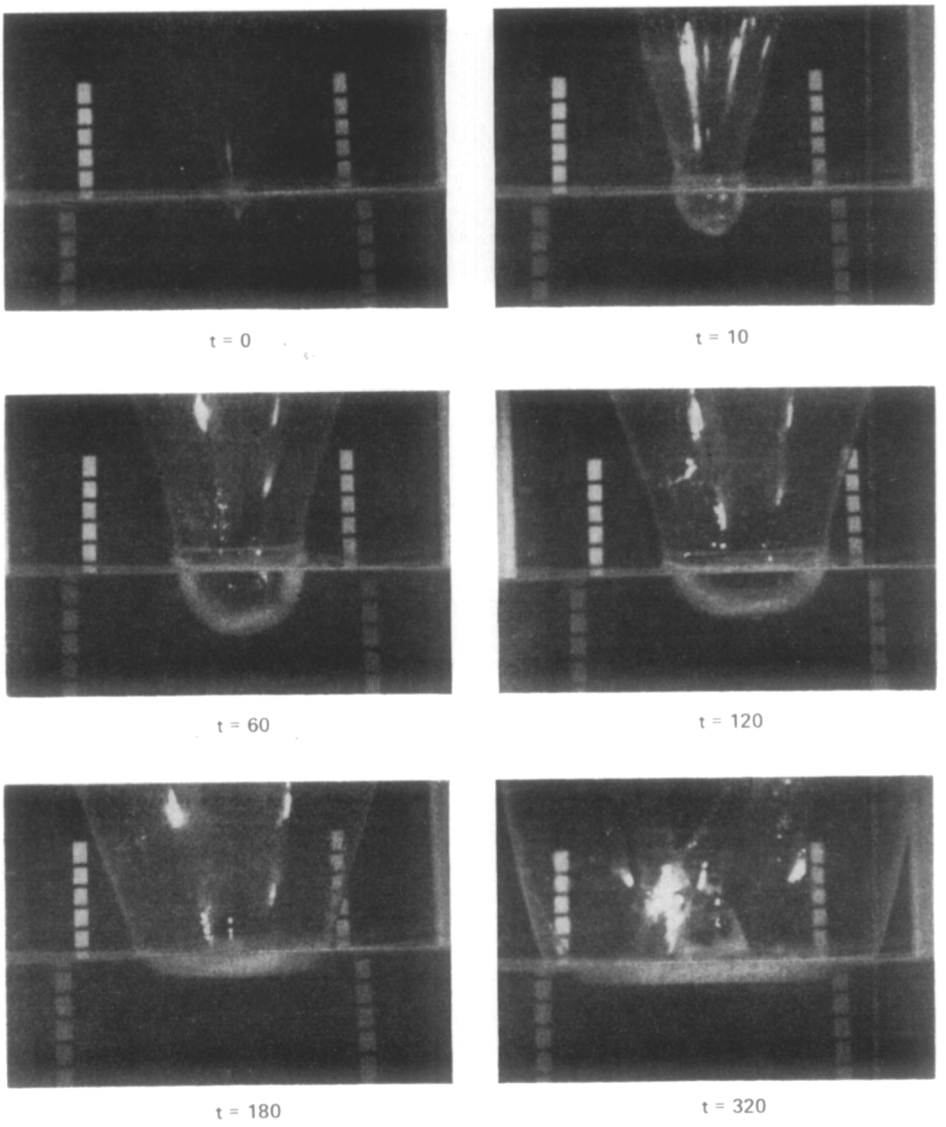

FIG. 6. Selected frames from a 16-mm movie record of a 1.59-mm-diameter Pyrex sphere impacting water at normal incidence with a velocity of approximately 2.5 km/sec (Round VGP 1610). Note the absence of holes or tears in the ejecta plume and the development of the hemispherical cavity that subsequently begins to collapse before the crater attains its maximum diameter and produces the large prominent central peak shown in the last picture of the sequence. Fiducial marks in the background are spaced at 5 cm. Time t shown in milliseconds after impact.

displayed by the full scale structures (e.g., Fig. 1). However, the experimental results shed light on the behavior of fluidized ejecta in the Martian environment, whether the Martian conditions involved subsurface water or melted ice entrained in ejecta, or atmospheric gas entrapped in the ejecta.

Scaling from tens of centimeters to tens of kilometers is recognized to be, at best, a tenuous extrapolation, but these explora-

tory experiments provide three key results that should be independent of scale:

(1) Decreasing viscosity (or increasing fluidity) promoted postdepositional flow in the ejecta.

(2) Decreasing viscosity increased the radial extent of the "continuous" ejecta deposits.

(3) The postdepositional flows exhibited apparent multiple ejecta flow units.

These results are attributable to the use of an "appropriate" value of target viscosity *at the scale of the experiment.* A direct quantitative extrapolation of the same "appropriate" value of viscosity to the Martian craters obviously would be incorrect. Materials with identical viscosity on Mars would be incapable of producing and sustaining the large scarps and ridges displayed in the Viking Orbiter images.

The establishment of the flows, both at model scale and full scale, should be expected to depend on the relative values of inertial forces (arising from the mass and velocity of the ejecta), and to the forces resisting the mass movement (arising from an effective viscosity of the ejecta). This suggests a relationship similar to the dimensionless ratio Reynolds number N_R which is commonly used in fluid mechanics to characterize the conditions of flows of viscous fluids.

$$N_R = \rho V d/\mu,$$

where ρ is the mass density of the fluid, V is the velocity of the fluid flow, d is some characteristic dimension of the flow, and μ is the viscosity of the fluid. However, direct application of N_R to the present case cannot be made because it would infer the fluidized material behaved as a Newtonian liquid. It is most probable, as indicated by flow morphologies, that the fluidized masses (both model and full scale) behaved as a Bingham-type liquid; that is, the flows acted as liquids having finite yield strengths. Stressed below the yield point there is no strain, but once a Bingham liquid is stressed above its yield point it then flows as a Newtonian liquid in that the shear stress is proportional to the rate of shear. The existence of a finite yield stress is essential for the observed flow morphologies. Without a finite yield stress, the terminal ridges and escarpments along the flow fronts could not be sustained. A modified form of the Reynolds number is, therefore, indicated which might include the yield strength τ

$$N_{Rm} = 1/(\mu/eVd + c\tau/\rho V^2),$$

where c is a constant. The appropriate measures for the six terms for present applications is a subject for separate and future discussion, but these preliminary experiments suggest that there could be a critical effective value for N_{Rm} below which no ejecta flow will occur. Large effective viscosities and high yield strengths, either individually or in combination, would cause the ejecta to be incapable of postdepositional flows. There will be an upper limit for N_{Rm} beyond which extreme fluidization resulting from vanishingly small viscosities and strengths (e.g., water for these experiments) would preclude preservation of flow structure and morphology. With this premise it would be possible to realize fluidization of large scale flows with materials having much greater viscosities and yield strengths than the simple mud materials of these exploratory experiments, a possibility that is plausible from both practical and physical considerations. Additionally, one can speculate that flows should be more prevalent and better developed with increasing distance from a crater due to the greater ballistic velocities required to transport the ejecta. This speculation has two implications, first, conditions favorable for ejecta flows will exist throughout a major fraction of the deposits around large craters while, second, the occurrence of flows around smaller craters would be most favorable at the outer margins of the

continuous deposits. In both cases, it would be expected that the flows would include material derived locally both by excavation during secondary impact and by the subsequent scouring action of the fluidized sheet as it flows radially outward from the crater (Oberbeck *et al.*, 1974). Scouring should be a particularly effective mechanism for sustaining and extending flows if subsurface water and/or ice were present and incorporated into the flows.

ACKNOWLEDGMENTS

We thank Paul Spudis, V. R. Overbeck, and an anonymous individual for helpful reviews of the original manuscript. Special thanks go to John Wedekind and Larry Robello for their invaluable help with the experiments.

Note added in proof. In preparation for additional experimentation, mixtures of soupy muds, thought to be similar to those described in the main text, yielded viscosities of the order 10^2 and 10^3 poise for, respectively, the syrup-like and wet-concrete-like muds. These values and estimates of yield strengths give a critical value for the Reynolds number N_{Rm} between 0.5 and 1.5/cm reference length. Based on this preliminary determination of viscosities, we estimate for a 10-km-diameter Martian crater that the requisite viscosities for the ejecta flows must be greater than 10^4 and possibly approach 10^5 poise, values which are in the same range as terrestrial debris and lava flows.

REFERENCES

ARVIDSON, R. H., CARUSI, A., CORADINI, A., CORADINI, M., FULCHIGNONI, M., FEDERICO, C., FUNICELLO, R., AND SALOMONE, M. (1976). Latitudinal variation of wind erosion of crater ejecta deposits on Mars. *Icarus* **27**, 503–516.

CARR, M. H., MASURSKY, H., BAUM, W. A., BLASIUS, K. R., BRIGGS, G. A., CUTTS, J. A., DUXBURY, T., GREELEY, R., GUEST, J. E., SMITH, B. A., SODERBLOM, L. A., VERVERKA, J., AND WELLMAN, J. B. (1976). Preliminary results from the Viking Orbiter imaging experiments. *Science* **193**, 766–776.

CARR, M. H., CRUMPLER, L. A., CUTTS, J. A., GREELEY, R., GUEST, J. E., AND MASURSKY, H. (1977). Martian craters and emplacement of ejecta by surface flows. *J. Geophys. Res.* **82**, 4055–4065.

GAULT, D. E., QUAIDE, W. L., AND OBERBECK, V. R. (1968). Impact cratering mechanics and structures. In *Shock Metamorphism of Natural Materials* (B. French and N. Short, Eds.), pp. 87–99. Mono Book Corp., Baltimore, Md.

GAULT, D. E., QUAIDE, W. L., AND OBERBECK, V. R. (1966). Luna 9 photographs: Evidence for a fragmental surface layer. *Science* **153**, 985–988.

GAULT, D. E., HÖRZ, F., AND HARTUNG, J. B. (1972). Effects of microcratering on the lunar surface. *Proc. Third Lunar Sci. Conf.* **3**, 2713–2734.

GAULT, D. E., HÖRZ, F., BROWNKE, D. E., AND HARTUNG, J. B. (1974). Mixing of the lunar regolith. *Proc. Fifth Lunar Sci. Conf.* **3**, 2365–2386.

HEAD, J. W., AND ROTH, R. (1976). Mars pedestal crater escarpments: Evidence for ejecta related emplacement. In *Symposium on Planetary Cratering Mechanics*, pp. 50–52. The Lunar Science Institute, Houston, Texas.

MCCAULEY, J. W. (1973). Mariner 9 evidence for wind erosion in the equatorial and mid-latitude regions of Mars. *J. Geophys. Res.* **78**, 4123-4137.

OBERBECK, V. R., MORRISON, R. H., HÖRZ, F., QUAIDE, W. L., AND GAULT, D. E. (1974). Smooth plains and continuous deposits of craters and basins. *Proc. Fifth Lunar Sci. Conf.* **1**, 111–136.

QUAIDE, W. L., AND OBERBECK, V. R. (1968). Thickness determinations of the lunar surface layer from lunar impact craters. *J. Geophys. Res.* **73**, 5247–5270.

STÖFFLER, D., GAULT, D. E., WEDEKIND, J. A., AND POLKOWSKI, G. (1975). Experimental hypervelocity impact into quartz sand: Distribution and shock metamorphism of ejecta. *J. Geophys. Res.* **80**, 4062–4077.